Izvestiya, Earth Physics
Physica of the Solid Earth
Vol. 20, No. 1, 1984

Quasi-Three-Dimensional Modeling of Magnetotelluric Fields in the Southern Turanian Plate and the South Caspian Megabasin

B. SH. ZINGER, V. G. DUBROVSKIY, E. B. FAYNBERG, M. N. BERDICHEVSKIY, AND K. IL'AMANOV

Institute of Earth Magnetism and Radiation, USSR Academy of Sciences;
Institute of Geology, Turkmenian SSR Academy of Sciences;
Moscow State University

A method is described and the results of numeric modelling of magnetotelluric fields in the southern Turanian plate and the South Caspian megabasin are given. One possible explanation of the magnetotelluric field anomaly established here could be the distorting influence of near-surface nonuniformities. An important contribution to the formation of the regional characteristics of magnetotelluric fields is made by the leakage of current through the conducting basement or faults.

Magnetotelluric field anomalies have been discovered in many regions of the earth. Some of these are attributed to the existence of intermediate conduction layers in the earth's crust and upper mantle at depths of 10 - 20 to 100 - 200 km.

A formal interpretation of experimental data is usually complicated by the presence of a nonuniform sedimentary cover. Until recently, the common way of taking into account the distorting effects of near-surface nonuniformities was comparison with well-studied two-dimensional models [1, 2]. The limitations of this approach are clear, because real horizontally nonuniform media cannot always be interpreted as two-dimensional entities.

Further progress in the interpretation of deep magnetotelluric soundings is largely predicted on developing the methods for computation of electromagnetic fields in three-dimensional nonuniform media. In this paper, we report the results of a numerical simulation of fields for a region encompassing the southern Turanian plate and the South Caspian megabasin. In that region, the Laboratory of Magnetotelluric Studies of the Institute of Seismology, and later the Institute of Geology of the Turkmenian SSR Academy of Sciences, conducted explorations for several years, resulting in ample data covering manifestations of boundary, induction, S-effects, and channeling (concentration) effects, that is, virtually all known types of distortions which often prevent a satisfactory interpretation of empirical results. The calculations proceeded from a quasi-three-dimensional model, where lateral nonuniformities are contained in a near-surface nonuniform thin layer, while the deep portion of the profile is represented by a conductor with electric conductivity depending only on depth. The iterative methods for calculation of electromagnetic fields in such models proposed until now have serious limitations as regards their applicability in terms of frequency range and variation rate of integral conductivity [3, 4], or in terms of the subjacent profile [5, 6]. Noteworthy direct methods of solution of the field equations have been proposed in [7, 8], but, regrettably, they do not provide sufficient detail of calculations.

The results of simulation reported here have been obtained with a program developed by the Institute of Earth Magnetism and Radiation of the USSR Academy of Sciences. The program is based on an iterative procedure first reported in [9]. For a more detailed description of the method and its generalizations, the reader is referred to [10 - 12]. An obvious advantage of this approach is the absence of any basic restrictions to applicability, either in terms of frequency range of the emitter field or as regards the spatial characteristics of the distribution of integral conductivity of the nonuniform thin layer. In substantiating the method and its practical applications modeling the global current systems induced in the real World Ocean and sedimentary cover [13], a general spherical model of the earth was used. Because the two-dimensional model can be viewed as a limiting case of a spherical model, all formulas of [9 - 12] and the substantiation of the iterative procedure are valid for the plane model as well, which is more convenient when modelling local or regional magnetotelluric fields. For that reason, we give only a brief presentation of the basic formulas in the following section.

The method for modeling the distorting effects of near-surface nonuniformities. Proceeding from the fundamental idea proposed by Swiatnamn [14] and Price [1], we assume that the spherical layer of near-surface nonuniformities is sufficiently thin to allow the variation of the structure of

current distribution across the layer to be disregarded. This assumption is realistic in the frequency range used for deep electromagnetic sounding. In this range, the tangential components of the electric field E_s and the normal component of the magnetic field H_n are virtually invariable across the layer, while the tangential components of the magnetic field experience the jump

$$\delta \mathbf{H}_s = -[\mathbf{n}, \mathbf{j}^{sur}],$$

determined by the surface current density (in the film)

$$\mathbf{j}^{sur} = S\mathbf{E}_s.$$

Here S is the integral conductivity of the thin layer. The medium lying under the sedimentary cover is assumed to be laterally uniform and to have the conductivity σ, depending solely on the depth. The distribution of the current density in such medium can be described in terms of the Debye potentials* V and W of toroidal and polhodal modes, respectively [12]:

$$\mathbf{j} = -i\omega\mu_0 \operatorname{curl}(\mathbf{n}\sigma V) + \operatorname{curl}\operatorname{curl}(\mathbf{n}W).$$

Here $\mathbf{n}$ is a unit vector normal to the surface of the thin layer, and ω is the frequency of the electromagnetic field. The expressions for the field components are

$$\mathbf{E}_s = i\omega\mu_0[\mathbf{n}, \nabla_s]V + \sigma^{-1}\nabla_s \frac{\partial W}{\partial n},$$

$$H = \mathbf{n}\Delta_s V - \nabla_s \frac{\partial V}{\partial n} - [\mathbf{n}, \nabla_s]W.$$

The differential operators with the subscript s refer to the corresponding surface differential operators. In the medium subjacent to the field, the Debye potentials obey the equations

$$\left(\frac{\partial^2}{\partial n^2} + \nabla_s^2 + i\omega\mu_0\sigma\right)V = 0,$$
$$\left(\frac{\partial}{\partial n}\sigma^{-1}\frac{\partial}{\partial n} + \sigma^{-1}\nabla_s^2 + i\omega\mu_0\right)W = 0. \quad (1)$$

The surface current density is determined by the jump of the derivative of the toroidal Debye potential normal to the layer,

$$\Psi = \delta\frac{\partial V}{\partial n},$$

usually referred to as the current function, and by the value assumed at the surface by the polhodal Debye potential W:

$$\mathbf{j}^{sur} = -[\mathbf{n}, \nabla_s]\Psi - \nabla_s W. \quad (2)$$

The distribution of the surface and volume currents can be found from solution of the equation system [12]:

$$\operatorname{div}_s \frac{\nabla_s\Psi - [\mathbf{n}, \nabla_s]W}{S} = -i\omega\mu_0\Delta_s V,$$
$$\operatorname{div}_s \frac{[\mathbf{n}, \nabla_s]\Psi + \nabla_s W}{S} = -\sigma^{-1}\Delta_s \frac{\partial W}{\partial n}. \quad (3)$$

The values of all variables in this system are taken on the surface of the thin layer.

The presence of the second term in (2), as well as of the second equation in (3), accounts for the possibility of leakage of current from the surface nonuniform layer into the subjacent section. Indeed, the value of the W potential on the thin layer determines the current leakage, because the normal component of current density,

$$j_n = -\Delta_s W.$$

Equations system (3) allows us to obtain an estimate of the significance of current leakage

$$f_L \sim \frac{\lambda j_n}{j^{sur}} \sim \left(1 + \frac{S}{\sigma\lambda_p}\right)^{-1}\frac{\lambda|\nabla S|}{S}.$$

By λ here we denote the characteristic distance of the variation of surface conductivity, and by λ_p the penetration depth of polhodal current mode.

If $f_L \ll 1$, only eddy current mode exists in the film, which is described by the current function Ψ. In that case, the first equation of system (3) becomes the well-known Price equation [3]. The general method of solution of induction equations in nonuniform media proposed in [9 - 12] can be conveniently applied to find the solutions of the integral form of system (3):

$$\Psi = \Psi_0 + \oint Q_\tau \operatorname{div}_s\left\{\frac{R'}{R_0}(\nabla_s\Psi - [\mathbf{n}, \nabla_s]W)\right\}ds',$$
$$W = \oint Q_n \operatorname{div}_s\left\{\frac{R'}{R_0}([\mathbf{n}, \nabla_s]\Psi + \nabla_s W)\right\}ds'. \quad (4)$$

The integration is done on the surface of the thin layer. By R', we denote the deviation $R' = S^{-1} - R_0$ of the inverse integral conductivity from a certain constant level R_0. Ψ_0 is the solution of system (3), with the same external field and subjacent section for the thin layer with integral

*We use the terminology commonly applied to descriptions of fields in spherical earth models. For the two-dimensional model, the V potential describes the behavior of the transverse-electrical mode, and the W potential, the transverse-magnetic mode.

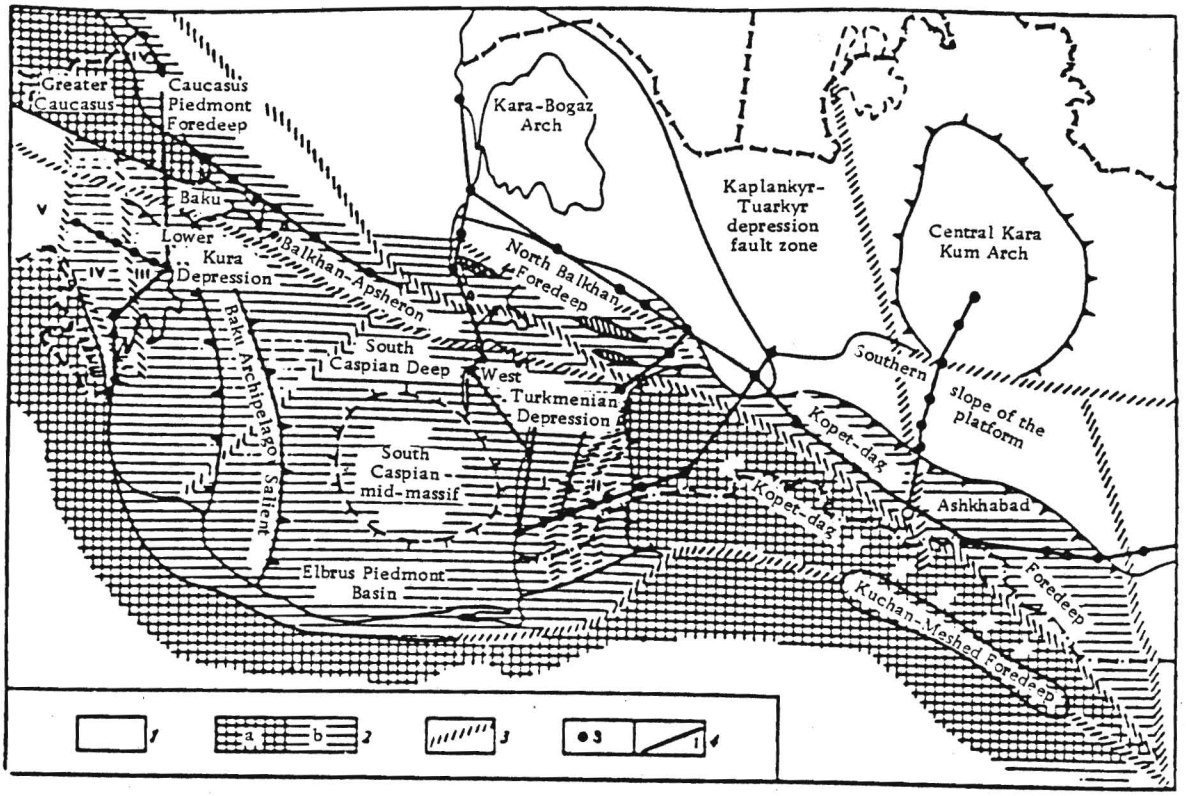

Fig. 1. Tectonic map of southern Turanian plate and South Caspian basin: 1) Epihercynian platform; 2) folded structures (a), depressions and foredeeps of Alpine orogenic system (b); 3) deep faults; 4) sites and observation profiles of DMTS; I) Gorandag-Chikishlyar level of the West Turkmenian basin; II) Aladag-Messeri level of the West Turkmenian basin; III) Shirvan tectonic zone of Lower Kura basin; IV) Mugan tectonic zone of Lower Kura basin.

conductivity R_0^{-1}. System (3) can be solved by an iterative procedure. The ratio of the two subsequent increments of the potential is a majorant with the quantity $\max|R'/R_0|$, which can always be made smaller than 1 by an appropriate choice of R_0.

In performing numerical calculations, one is faced with limited resources (especially, the operation speed and the working memory capacity of the existing computers). This often prevents field calculations from being performed with the degree of detail that is necessary for practical purposes. An advantage of the method is the possibility of a consecutive increase of detail of calculation of the electromagnetic field covering the region of interest.

Indeed, as a natural first step, we calculate the field for the spherical earth model, taking into account only the global and major regional features of the distribution of near-surface conductivity. In that case, $\mathcal{S}$ does not include the details that cannot be represented in the calculation grid being used; the distribution is obtained in a smoothed form, and the fields can be called normal. At the next stage, we compute the deviations $\Psi_a=\Psi-\Psi_n$, $W_a=W-W_n$ that account for "finer" features $R_a=S^{-1}-R_n$ of the sedimentary cover in the particular area concerned. To find them, we use the same iterative procedure to solve the system of integral equations flowing from (4):

$$\Psi_a=\Psi_a^{\cdot}+\int_{\cdot} Q_r \operatorname{div}_s\left\{\frac{R'}{R_0}(\nabla_s\Psi_a-[\mathbf{n},\nabla_s]W_a)\right\}ds',$$
$$W_a=W_a^{\cdot}+\int_{\cdot} Q_r \operatorname{div}_s\left\{\frac{R'}{R_0}([\mathbf{n},\nabla_s]\Psi_a+\nabla_s W_a)\right\}ds', \quad (5)$$

where

$$\Psi_a^{\cdot}=\int_{\cdot} Q_r \operatorname{div}_s\left\{\frac{R_a}{R_0}(\nabla_s\Psi_n-[\mathbf{n},\nabla_s]W_n)\right\}ds',$$
$$W_a^{\cdot}=\int_{\cdot} Q_r \operatorname{div}_s\left\{\frac{R_a}{R_0}([\mathbf{n},\nabla_s]\Psi_n+\nabla_s W)\right\}ds'.$$

If necessary, one can proceed to the next

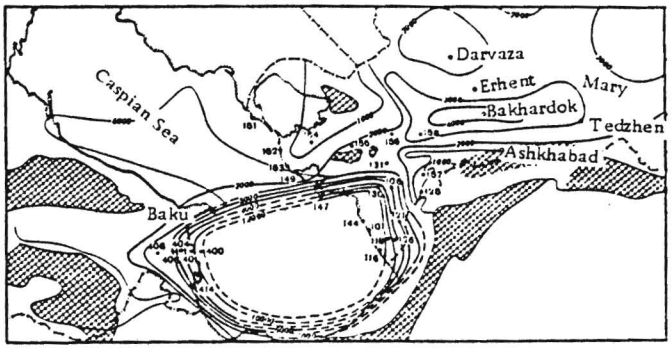

Fig. 2. Total longitudinal conductivity of sedimentary cover around central Turkmenian and South Caspian Megabasins. Isolines correspond to values in mhos. Dots show observation sites.

degree of detailed calculations, etc. The final stage takes into account the influence of near-surface nonuniformities of a limited area, and one can disregard the influence of sphericity and use a two-dimensional earth model. The nuclei of integral transformations (5) for the plane model appear as

$$-2\pi Q_T'(r)=\frac{1}{r}+\int_0^\infty \frac{i\zeta_k}{1-i\zeta_k}J_1(kr)\,dk, \qquad \zeta_k=\omega\mu_0\frac{\alpha_k(\omega)}{2k}$$

$$-2\pi Q_P'(r)=\frac{1}{r}-\int_0^\infty \frac{\xi_k}{1+\xi_k}J_1(kr)\,dk, \qquad \xi_k=\frac{\beta_k(\omega)}{\sigma(0+0)R_0}.$$

Here $J_1(z)$ is the standard notation for the first order Bessel function; $\alpha_k(\omega)$ and $\beta_k(\omega)$ are impedance functions determined by the stratified profile subjacent to the film; $\alpha_k(\omega)-1$ is the ratio of the internal portion of the Debye potential of the toroidal mode to the external portion; and $\beta_k(\omega)$ is the logarithmic normal derivative of the polhodal Debye potential on the cap rock for the respective surface harmonic e^{ikr/R_0}. The method described in this section provides a convergence of the iterative process at any frequency ω of the emitter field and any pattern of distribution of integral conductivity of the thin layer.

Brief description of the region [16]. The territory under study is subdivided by geological and geophysical features into two parts: the southern Turanian plate and the South Caspian megabasin (Fig. 1).

Within the southern Turanian plate, two uplifts of the crystalline basement are identified: the central Kara Kum arch with a sedimentary thickness of 1600 - 2000 m, and the Kara Bogaz arch with sediments about 1000-m thick. The central Kara Kum arch is separated from the folded structures of the Kopet-Dag by the southern slope of the Kara Kum platform and the Kopet-Dag fore-

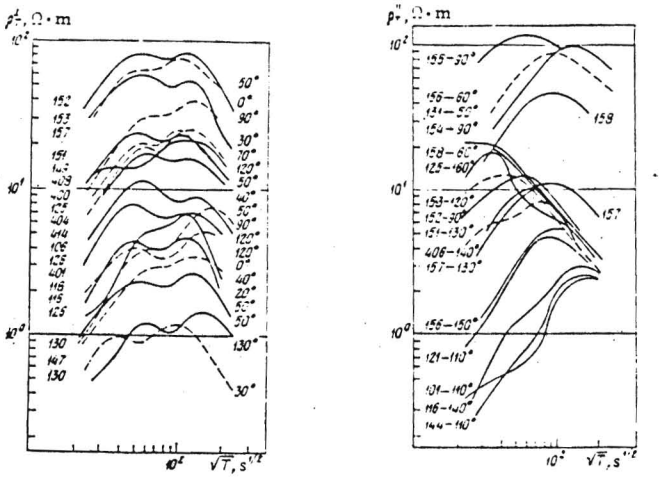

Fig. 3. Experimental curves of ρ_T: a) type I; b) type II. Numbers at curves give observation sites and directions of the principal axis of impedance diagram for which the ρ_T curve is plotted.

deep. The Kara Bogaz arch encompasses the Kara-Bogaz Gol Bay, the northern Krasnovodsk Peninsula, and the adjacent part of the middle Caspian Sea. The basement generally subsides in a southeastern direction to depths of ~3-4 km.

The South Caspian megabasin occupies a large area, including the western Turkmenian and Kura lowlands and the southern part of the Caspian Sea. Generally, the megabasin is a huge area bounded on the south by the Elburz mega-anticlinorium and Talysh Ridge and on the west by structures of the Greater and Lesser Caucasus. East of the West Turkmenian lowland is the piedmont of West Kopet-Dag. In the West Turkmenian lowland, as well as the South Caspian basin, the sedimentary thickness

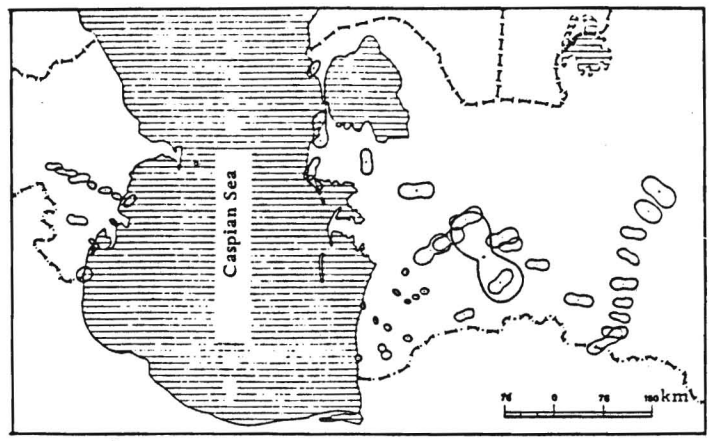

Fig. 4. Map of diagrams of principal impedance moduli for variation period of 6 h.

attains 25 km. The sedimentary thickness in the Lower Kura lowland is about 16 to 18 km. A diagram of composite longitudinal conductivity of the sedimentary cover based on electric prospecting data is shown in Fig. 2. It is seen that, within the territory studied, S varies in a broad range. The southern Turanian plate has a relatively stable $S \sim 2000 - 4000$ mhos, while the northern border of the megabasin, about 1000 mhos. Within the megadepression, S attains 13,000 mhos. In the mountain areas, the value of S = 100 mhos was assumed by way of convention. No reliable data on the conductivity of sedimentary cover in these areas are available.

Features of the magnetotelluric field [15, 16]. The magnetotelluric field was measured here along a series of profiles crossing the territory in different directions. The measurement sites and the resulting ρ_T curves are shown in Figs. 2 and 3.

The curves of apparent resistivity obtained from interpretation of empiric data are subdivided into two types. The curves of $\rho_T^{\perp}$, belonging to the first type, are observed in the megabasin and on its northern margin for submeridional ($30 \pm 30°$) polarization of the telluric field, i.e., across the course of the northern margin of the megabasin. As S varied from 1000 to 13,000 mhos, the shape of the curves was largely retained, while the readings varied by almost two orders of magnitude (Fig. 3a). An important feature of the first type of curves is the bend with a minimum of 1.5 - 2.0 h.

The curves of the second type, $\rho_T^{\parallel}$ (Fig. 2b) are mostly observed with sublatitudinal ($120 \pm 30°$) polarizations of the telluric field. As seen from the figure, they have a "one-hump" shape and are subdivided into two subgroups by the level of descending asymptotes. The curves of the first group were obtained in the southern Kara Kum platform, and the second subgroup inside the megabasin and on its northern margin. The asymptote to which the curves of the first group tend is close to the global curve of apparent resistivity. The descending asymptote of the second group lies an order of magnitude below the first one.

The general pattern of behavior of the field in the region is well illustrated by the map of polar diagrams of the principal impedance moduli on the period of 6 h (Fig. 4). Obviously, the major factor determining the behavior of the magnetotelluric field in Central Turkmenia is the high-resistivity mountain borders of the southern Turanian plate. The polar diagrams here are extended in a sublatitudinal direction (across the strike of the Kopet-Dag).

The telluric field component directed across the Kopet-Dag is attenuated by the boundary effect that is increased as one approaches the mountains. The mean values of ρ_T for this region are shown by the curves in Fig. 5a. The curves that are transverse in relation to Kopet-Dag are seen to lie almost an order of magnitude below the longitudinal curves, indicating the boundary effect. In the Kubadag-Greater Balkhan zone, the polar diagrams turn, showing that the currents flow around the Kubadag and Greater Balkhan Mega-anticlinorium. The mean ρ_T curves for these zones are shown in Fig. 5b.

On the northern margin of the megabasin, the polar diagrams turn almost orthogonally relative to their position in Central Turkmenia. The longitudinal values of $\rho_T^{\parallel}$ are almost an order of magnitude smaller than $\rho_T^{\perp}$ despite the absence of any obstacles to current flows in the sublatitudinal direction (Fig. 5c). Inside the megabasin (Fig. 5d), impedances are seen to drop almost everywhere regardless of the direction of the telluric field.

An interpretation of the longitudinal curves of magnetotelluric sounding in the South Caspian

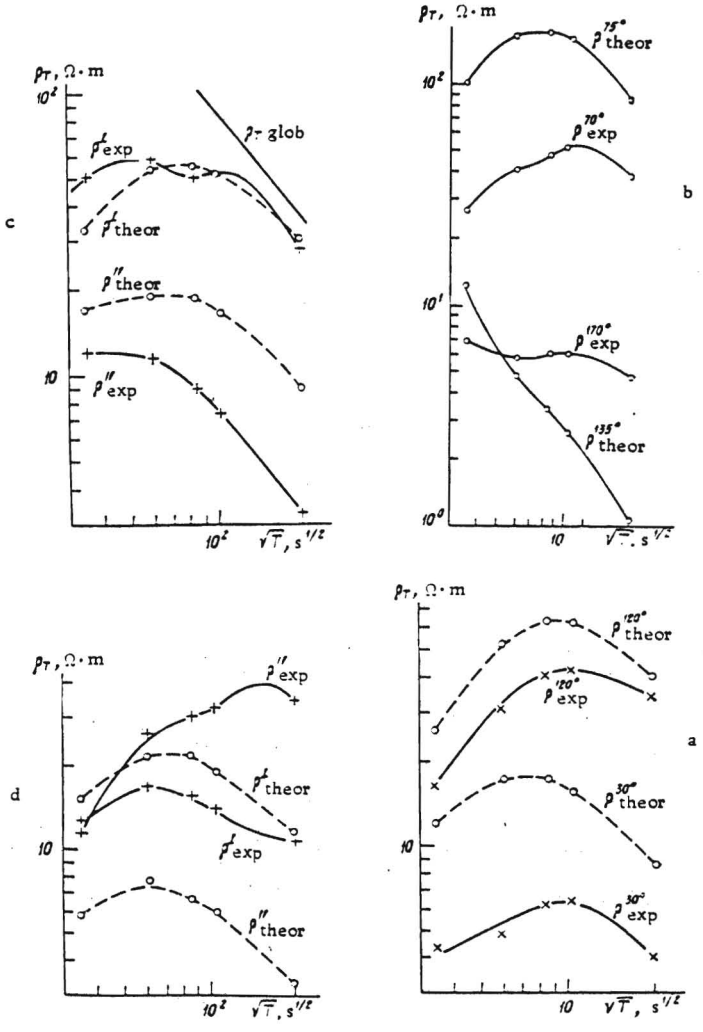

Fig. 5. Experimental and model ρ_T curves: a) southern slope of Kara Kum platform, b) Kubadag-Greater Balkhan and western Kopet-Dag zones, c) northern wall of the megabasin, d) South Caspian megabasin.

megabasin was offered in [15]. The decline of the telluric field up to 10 or 30% compared with the field in Central Turkmenia, according to that interpretation, was attributed to the existence, at a depth of 50 - 60 km, of a highly conducting, up to 20-km thick layer with a resistivity of about 1 Ω·m.

The first quasi-three-dimensional modelling of telluric fields in the South Caspian megabasin and neighboring territories was done by Van'yan, Dubrovskiy, Yegorov, and Konnov [17]. Disregarding the effects of self- and reciprocal induction, they computed the telluric fields in nonuniform thin layer S, simulating the distribution of total longitudinal conductivity of the sedimentary cover. When the calculation data were fitted to impedance distribution maps, a qualitative agreement was observed. In particular, the calculations revealed the boundary effect at the platform and an attenuation of the telluric field in the megabasin. This result suggested that the low telluric field in the megabasin may be induced by regional field distortions rather than a conducting layer in the megabasin. This interpretation requires further elaboration. In particular, calculations are needed that would take into account the induction effects in the presence of normal deep profiles and a comparison of the empiric data and numeric modelling at the level of ρ_T curves that would take into consideration the tensor nature of the impedances. These calculations have been performed using the method described earlier.

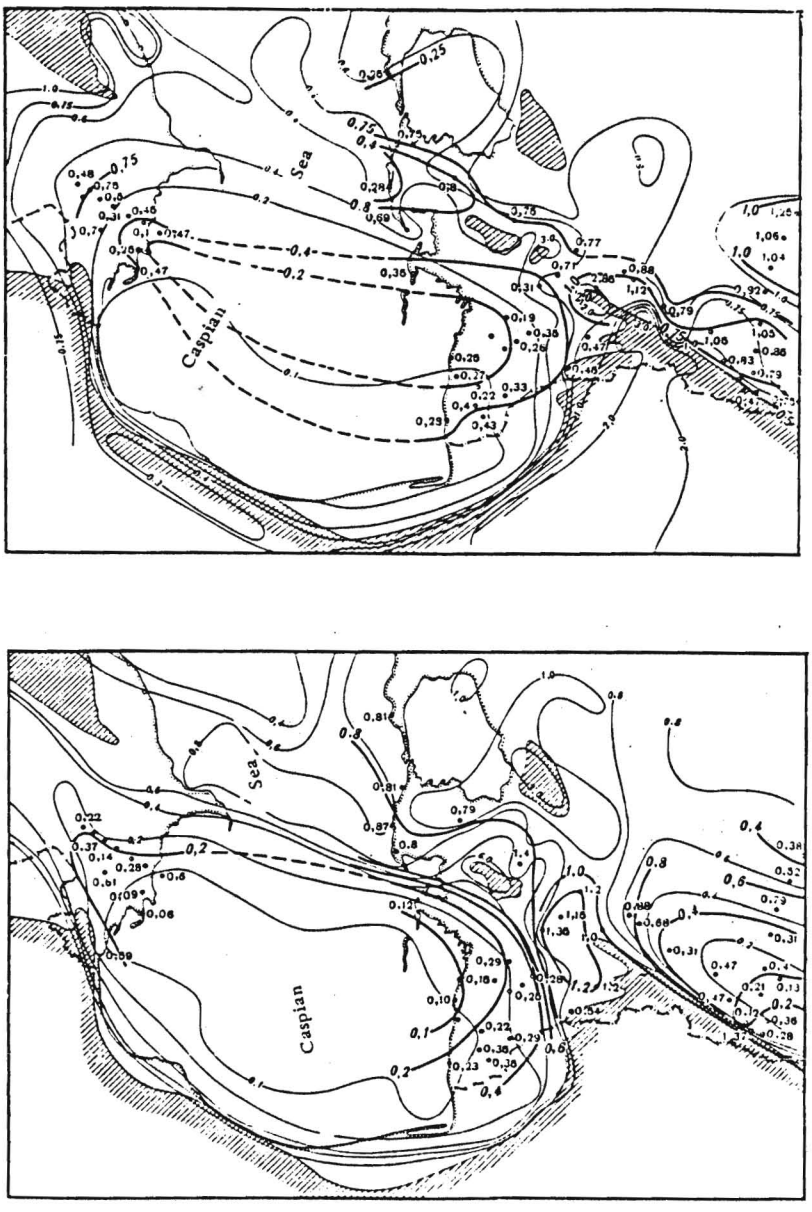

Fig. 6. Spatial distribution of experimental impedance (thick lines) and model impedance (thin lines) for a period of 12 h. Numbers at circles give experimental impedance values at observation sites; a) sublatitudinal telluric field polarization, b) submeridional telluric field polarization.

Choice of model. We take for the normal the profile defined in [16] in the framework of two-parameter power model $\sigma=\sigma_0(h/h_0)^\gamma$, with h_0 = 1 km. The model parameters based on interpretation of longitudinal curves from the southern Turanian plate are $\sigma_0 = 0.25 \times 10^{-7}$ mhos/m and $\gamma = 2.593$, respectively. The distribution is average for the southern Turanian plate. Similar values of σ_0 and γ have been obtained from interpretations of global data in [18]. This deep profile was used for modeling in all regions under study.

The results of modeling of global current systems [13] indicate, in particular, that the normal current function has almost constant gradients, with the predominant polarization of the

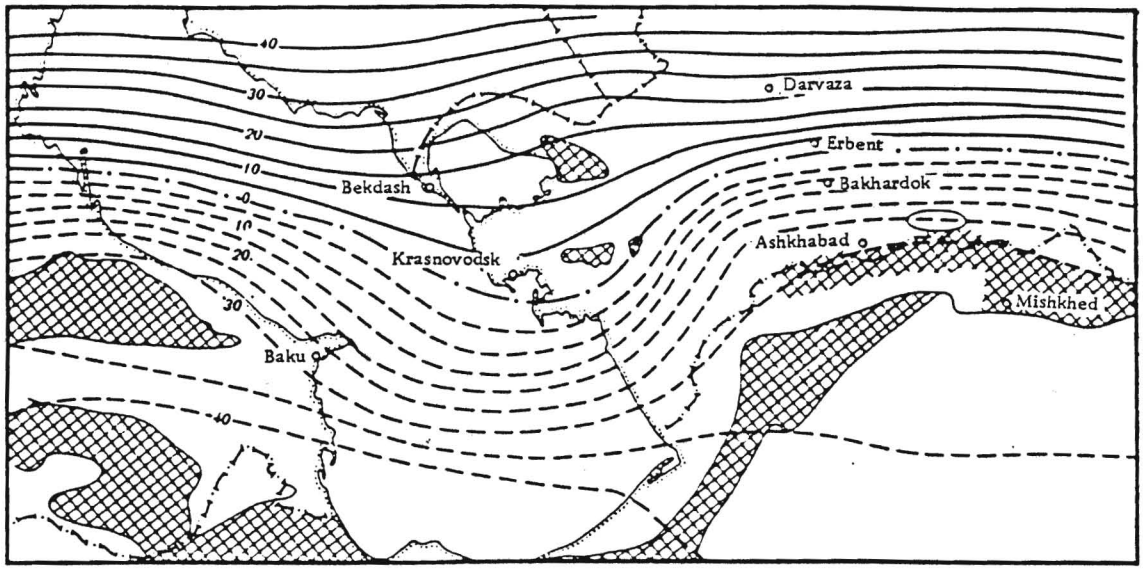

Fig. 7. Current system induced in the near-surface conducting layer for a 12 h period with sublatitudinal telluric field polarization. Isolines of current function are in relative units.

telluric field along the Greater Caucasus—Kopet-Dag line. This allowed taking for the normal conductivity level S_n = 2000 mhos, a value close to average for the southern Turanian plate. The coordinate system was chosen with axes coincident with the directions of the Kopet-Dag's course and dip.

The results of numeric modeling of magnetotelluric fields. The territory was divided into 25-km squares; it occupied the central portion of the transparency. The integral conductivity of the surrounding territory was equal to the normal S_n. The model was activated by a plane wave. The calculations were done for variations with periods of 20 min, and 1, 2, 3, 6, and 12 h.

A direct comparison of model and experimental MT-fields was impossible because of the absence of synchronic measurements. For that reason, normalized impedances were compared for two principal directions: along and across the Kopet-Dag. Normalization was done for impedances Z_n in the area of the southern slope of the Kara Kum platform, where the curves were closest to the data of global soundings.

Figure 6 shows spatial distribution of $|Z^{\shortparallel}/Z_n|$ and $|Z^{\perp}/Z_n|$ on the period of T = 12 h for experimental and model impedances. It is seen from Fig. 6b that natural and model impedances $|Z^{\perp}|$, defined in the direction orthogonal to the course of the Kopet-Dag, were similar for the entire territory. As one approaches the Kopet-Dag boundary effect becomes increased in central Turkmenia. On the central Kara Kum arch, which lies at 100 km from the frontal Kopet-Dag Ridge, and telluric field is 50% lower. The patterns are remarkably similar inside the megabasin, on its southern margin and in the West Turkmenian and Kura lowlands. A comparison of Fig. 6b with Fig. 2 shows the telluric fields in the megabasin and on its northern margin are largely controlled by the local values of S. In the middle of the megabasin, the field is reduced tenfold compared with the baseline.

A different picture is observed for longitudinal polarization of the telluric field (Fig. 6a). The calculated and experimental data are close in the southern Turanian plate. Even details match, such as a drop of the telluric field with approach to the Kopet-Dag foredeep and a rise of the field on the western border of the front range of the Kopet-Dag. The modelling provided an explanation for the drop of the telluric field in the southern Turanian plate near the northern margin of the megabasin. The Kopet-Dag and the Greater Caucasus are linear elongated structures and there are no obstacles to the flow of currents along these structures. Modelling showed quite graphically that an attenuation of the electric field near the northern margin was due to the current flowing into the megabasin. Figure 7 shows the current function for a period of 12 h. We observe here manifestations of three-dimensional S-effects. Apparently, this is a natural effect that could be observed wherever the sedimentary cover includes nonuniformities. Unlike the two-dimensional S-effect that is manifested in a shift of the level of the ρ_T curve without modifying its shape, the three-dimensional S-effect may also lead to a shift of the extrema of the ρ_T curve.

Remarkably, the horizontal components of the magnetic field within the entire region vary slightly, with maximum range of variation never exceeding 20 to 30%.

For a complete comparison of the calculated and experimental data, model ρ_T curves were constructed for the principal impedance tensor components. The principal impedances were taken from polar diagrams. The calculated ρ_T values were combined for the same zones as the experimental data and then averaged. The match of the empiric and model ρ_T curves in Fig. 5 confirmed the conclusion made from the analysis of the spatial structure of the magnetotelluric field.

The South Caspian megabasin had an experimental field attenuation that was half the value obtained from the model. The West Turkmenian lowland had approximately equal impedance values, and the relationship to S was weak. The calculation, however, indicated a correlation between impedance and S in that area. This discrepancy is regional and could not be accounted for by calculation or experimental errors.

CONCLUSIONS

The results of calculation of the magnetotelluric field in a model consisting of an S-film simulating the sedimentary cover and underlain by a gradient profile common for the entire region made it possible to account for the major patterns of behavior of the magnetotelluric field in the southern Turanian plate and the South Caspian megabasin. There were, however, two discrepancies from the experimental results that were significant. First, the transverse ρ_T curves calculated for the megabasin and its northern margin had no minima. To account for the minima, one would probably have to use a more involved scheme of the deep portion of the profile in that area. Second, the calculations suggested a stronger decline of the field in the megabasin than what was observed in the experiment. The inclusion of a conducting layer under the megabasin into the deep profile would only intensify this discrepancy. The possible explanations seem to point to a modification of the model that would allow for the possibility of current overflow through the megabasin in the direction of the Greater Caucasus-Kopet-Dag axis. Channels of such leakage could be individual regional faults or a system of local sublatitudinal faults, the existence of conducting rocks south of the front ridge of the Kopet-Dag, or, finally, a low transverse resistivity of the basement rocks in the megabasin, which would allow a leakage of currents between the sedimentary cover and the subjacent strata. Any of these mechanisms would lead to conclusions of great importance for the geology and tectonics of the territory, suggesting that analysis of the magnetotelluric soundings in the area should be continued.

At present, no reliable data are available on the transverse resistivity of the cover over the crystalline basement. The available experimental estimates have a divergence of at least two or three orders of magnitude. On the other hand, calculations persistently suggest an important role of current leakage from the sedimentary cover into the subjacent rocks. The authors have made similar calculations for a model which, in addition to the region discussed here, included the Pamir and Tien Shan massifs. The results of calculations that failed to take into account leakage effects showed that the boundary effect from the Pamir and Tien Shan would weaken the telluric field in Central Turkmenia, which was not observed in the sublatitudinal polarization of the field. In [20], the results were reported of the calculation of impedance tensors in the range from 1 to 48 h based on modelling of global current systems [13]. The impedances obtained for the southern Turanian plate also had significantly lower values than experimental observations. Finally, the pattern of polar diagrams produced by experimental data in central and southeastern Turkmenia also suggest that Tien Shan is no serious obstacle to current overflow. It could be expected that either there are conducting layers under the Tien Shan, or that currents overflow through regional faults existing in that area.

In conclusion, distortions of the magnetotelluric field similar to those described here must certainly be widespread. This calls for performing calculations that would help clarify the role of near-surface distortions for all regions where magnetotelluric anomalies have been discovered.

Received November 16, 1982

REFERENCES

1. Berdichevskiy, M. N. Elektricheskaya razvedka metodam magnitotellurichesko go profilirovaniya (Electrical Prospecting by the Method of Magnetotelluric Profiling). Moscow, Nauka, 1968.
2. Dmitriyev, V. I., M. N. Berdichevskiy, and G. A. Kokotushkin. (Al'bom paletok dlya magnitotellurichesko go zondirovaniya v neodnorodnykh sredakh (Album of Transparencies for Magnetotelluric Sounding in Heterogeneous Media). Moscow, MGU Press, part 4, 1975.
3. Price, A. T. The induction of electric currents in nonuniform thin sheets and shells. Quart. J. Mech. Appl. Math., 2, 283-310, 1949.

4. Debabov, A. S. Numeric modelling of magnetotelluric field distortions by random surface nonuniformities, in Elektromagnitnyye zondirovaniya. Dokl. IV Vsesoyuzn. shkoly-seminara po elektromagnitnym zondirovaniyam. Zvenigorod, aprel' 1976. Ch. 1 (Electromagnetic Sounding. Papers at the Fourth All-Union Workshop on Electromagnetic Soundings. Zvenigorod, April 1976. Part 1). Moscow, pp. 61-63, 1976.
5. Hutson, V. D. L., P. C. Kendall and S. R. C. Malin. Computation of the solution of geomagnetic induction problem: A general solution with applications. Geophys. J. Roy. Astron. Soc., Vol. 28, 489-498, 1972.
6. Hobbs, B. A. and A. M. M. Brignall. A method for solving of electromagnetic induction in the oceans. Geophys. J. Roy. Astron. Soc., Vol. 45, 527-542, 1976.
7. Vasseur, G. and P. Weidelt. Bimodal electromagnetic induction in nonuniform thin sheets with application to the Northern Pyrenean induction anomaly. Geophys. J. Roy. Astron. Soc., Vol. 51, 669-690, 1977.
8. Dawson, T. W. and J. T. Weaver. Three-dimensional induction in a nonuniform thin sheet at the surface of a uniformly conducting earth. Geophys. J. Roy. Astron. Soc., Vol. 59, 445-462, 1979.
9. Fainberg, E. B. Electromagnetic induction in world oceans. Fourth Workshop on Electromagnetic Induction in the Earth and Moon. FGR, Murnay, Vol. 13-21, 1978.
10. Zinger, B. Sh. and E. B. Faynberg. Elektromagnitnaya induktsiya v neodnorodnoy tonkoy plenke (Electromagnetic Induction in a Nonuniform Thin Film). Preprint 13(242), IZMIRAN, 1979. Abstracted in RZh Geofizika, 8A16, 1979.
11. Zinger, B. Sh. and E. B. Faynberg. Electromagnetic field calculation in the World Ocean. Geomagnitizm i aeronomiya, Vol. 20, 106-110, 1980.
12. Zinger, B. Sh. and E. B. Faynberg. Electromagnetic induction in spherical nonuniform earth model. Izv. Akad. Nauk SSSR, Fizika Zemli, No. 5, 56-68, 1980.
13. Zinger, B. Sh. and E. B. Faynberg. Electromagnetic induction in nonuniform spherical earth model with real distribution of near-surface conductivity. Izv. Akad. Nauk SSSR, Fizika Zemli, No. 6, 59-64, 1981.
14. Sheynman, S. M. Stabilization of electrical fields in the earth, in Prikladnaya geofizika (Applied Geophysics). Moscow, Gostoptekhizdat, part 3, pp. 8-13, 1947.
15. Avagimov, A. A., T. Ashirov, V. G. Dubrovskiy and K. Nepesov. Deep Magnetotelluric Surveys in Turkmenia and Azerbaijan: Geoelectric and Geothermal Studies. Budapest, Akademiai Kiado, pp. 652-655, 1976.
16. Avagimov, A. A., T. Ashirov, M. N. Berdichevskiy, V. G. Dubrovskiy, Ye. V. Dubrovskaya, K. Il'amanov, L. P. Lagutinskaya, K. Nepesov, Ya. B. Smirnov, V. A. Sopiyev, O. M. Tavnelova and E. B. Faynberg. Geoelectric and thermal model of the deep structure of Southern Turanian Plate. Izv. Akad. Nauk SSSR, Fizika Zemli, No. 7, 15-28, 1981.
17. Van'yan, L. L., V. G. Dubrovskiy, I. V. Yegorov and Yu. K. Konnov. Structure of the low-frequency telluric fields of the South Caspian Megadepression based on numeric modelling. Izv. Akad. Nauk SSSR, Fizika Zemli, No. 7, 98-101, 1983.
18. Faynberg, E. B. Inverse problem of deep electromagnetic sounding of the earth. Geomagnitizm i aeronomiya, 21, No. 4, 715-719, 1981.
19. Zinger, B. Sh. Analytic solution of the problem of electromagnetic induction in nonuniform thin sheet. Geomagnetizm i aeronomiya, 22, No. 5, 887-889, 1982.
20. Faynberg, E. B., B. Sh. Zinger, and A. V. Kuvshinov. Electromagnetic fields induced in the World Ocean and spatial distribution of electrical conductivity functions. Physics Earth Planet. Inter., 32, No. 4, 8-15, 1983.